Rainfall-driven variations in $\delta^{13}C$ composition and wood anatomy of *Breonadia salicina* trees from South Africa between AD 1375 and 1995

Elin Norström[a*], Karin Holmgren[a] and Carl-Magnus Mörth[b]

This study demonstrates the potential of deriving palaeo-environmental information from carbon isotope composition ($\delta^{13}C$) and wood anatomy properties along the growth radii of two *Breonadia salicina* trees from Limpopo province, South Africa. An age model, based on AMS dating and 'wiggle-match' dating of the wood, shows that the data series from the two trees span AD 1375–1995 and 1447–1994, respectively. Shifts in the trees' $\delta^{13}C$ composition and wood anatomy resemble the indications of climate change observed in regional palaeoclimatic studies, and the parts of the *B. salicina* record from the last century show similarities with the observed variations in annual rainfall in the region. We propose that changes in carbon isotope composition and wood anatomy indicate variations in regional rainfall during the period of tree growth. Both the $\delta^{13}C$ and the wood anatomy records of *B. salicina* signify dry conditions in the early 1400s, mid-1500s, 1700s and early 1900s. The wettest conditions were during the late 1400s and in the 1600s.

Introduction

According to climatic predictions by the IPCC,[1] rainfall distribution in southern Africa will change during the next few decades; tropical regions are expected to receive more rain and subtropical regions less rain than today. However, there is a high degree of uncertainty associated with climate prediction models, as the inter-model variability is large for both tropical and subtropical regions of southern Africa. Despite indications of the significance of the tropics for global climate systems on various timescales (for example, refs 2–4), the dynamics of past climates of tropical and subtropical regions have not been studied, nor understood, as thoroughly as the palaeoclimate of temperate regions. During the last decade, however, the amount of high-resolution palaeoclimatic data from southern Africa covering the late Holocene has increased. Studies of speleothems,[5,6] pollen,[7] lake levels,[8] and trees[9] have contributed to valuable knowledge about past climatic change in the region. The spatial distribution of palaeoclimatic data is still sparse compared to that of temperate regions and a denser pattern of high-resolution data is needed in order to place regional climate change in a global context and to produce trustworthy climatic predictions.[10]

In dendroclimatology, different properties of annual tree rings (mainly width and density) are measured in order to extract palaeoclimate information with yearly resolution.[11] In tropical and subtropical regions, dendroclimatology is used to a lesser extent than in temperate regions, because of the weaker temperature and day-length seasonality, which results in fewer trees producing distinct annual rings. However, sometimes rainfall seasonality can trigger trees to produce annual growth structures in the wood. In southern Africa this is observed in only a few, mainly gymnosperm species, where ring formations are often difficult to identify and interpret.[12–14] In angiosperm trees, the rings may sometimes be identified by thin bands of parenchyma cells (thin-walled cells used mainly for storage and carbohydrate transport) or by gradual changes in the size of vessel cells (ring porosity).[12] Attempts have been made to apply dendroclimatology in southern Africa, but only a few have overcome the problem of cross-dating between trees.[9,15,16] These studies confirm that the use of dendrochronology and dendroclimatology in the tropics and subtropics is feasible, even though much more complicated, and more restricted in its time-extension, than in temperate regions.

A method complementary to ring-width analysis is the study of chemical properties, such as stable carbon, oxygen and hydrogen isotopes in tree rings. Using carbon isotope composition as a proxy for climate in trees is based on fractionations of the stable isotopes ^{13}C and ^{12}C during photosynthetic transpiration and carbon fixation.[17,18] The relation between ^{13}C and ^{12}C, expressed as the $\delta^{13}C$ value[a], is fixed within each growth ring, and each year a certain $\delta^{13}C$ signal is stored within the wood. As the magnitude of fractionation during photosynthesis is influenced by factors such as temperature, irradiation and soil moisture, the $\delta^{13}C$ variations in the tree rings may be used as a proxy for these climate-related parameters.[19–23]

Another way to retrieve climate information from trees is to analyse changes in wood anatomy, as the size and density of the water transporting cells (vessels) in certain angiosperm species change as a result of soil moisture status (for example, refs 24–26). This is an effective strategy for the tree, as only a small change in vessel diameter will affect the water conductivity dramatically, since the relationship between the factors is exponential[b]. Gillespie *et al.*[26] confirm a relationship between precipitation amounts and vessel properties for the same tree species investigated in this study, *Breonadia salicina*. This observation is promising for the use of this species as a palaeoclimate indicator.

In the study reported here, we analysed variations in carbon isotope composition and wood anatomy in two *B. salicina* trees from northern South Africa (Fig. 1). At the start of this project, our expectation was that the visible layers in the trees were seasonal growth rings, and that data with annual resolution could be extracted. AMS datings of the wood revealed, however, that the tree was much older than the ring counts indicated. Thus, although the possibility of obtaining data with annual resolution was lost, the potential of obtaining a climatic record spanning a longer time period was gained.

[a]Department of Physical Geography and Quaternary Geology, Stockholm University, 106 91 Stockholm, Sweden.
[b]Department of Geology and Geochemistry, Stockholm University.
*Author for correspondence. E-mail: elin.norstrom@natgeo.su.se

[a]The relation between the isotopes ^{13}C and ^{12}C is often referred to as $\delta^{13}C$, which expresses the plant isotope composition in relation to the isotope composition in a reference material, PDB. $\delta^{13}C_{plant} = [(R_{plant} - R_{ref})/R_{ref}] \times 1000$, where $R_{plant} = (^{13}C_{plant}/^{12}C_{plant})$ and $R_{ref} = (^{13}C_{PDB}/^{12}C_{PDB})$.

[b]The conductivity of water is proportional to the vessel diameter raised to the 4th power according to the Hagen-Poiseuille equation: $K_{capillary} = r^4\pi/8\eta$, where $K_{capillary}$ is the hydraulic conductivity, r is the vessel radius, and η is the viscosity of the sap.[27]

Fig. 1. Map of South Africa and neighbouring countries, showing major cities and important localities mentioned in the text.

Material and methods

Our study included $\delta^{13}C$ analysis of two specimens of *B. salicina*.[c] The species is common along permanent streams and rivers in riverine fringe forests from Tanzania in the north to KwaZulu-Natal in South Africa, where it is a protected species. This evergreen tree can reach 10–40 m in height and up to 2 m in stem diameter.[28] *B. salicina* requires large amounts of water and is frost-sensitive, but can endure occasional cold spells. When conditions are optimal, it may grow quickly — up to 1 metre in height per year.[29] The species shows vague annual rings and changes in xylem features are correlated with variations in precipitation.[26] As far as we know, there is no other detailed study on how *B. salicina* adapts, structurally and in terms of stomata-related responses, to external stimuli such as soil moisture.

The trees used in this study grew in the summer rainfall region of South Africa, in the eastern part of Limpopo province, 20 km southeast of the village of Tzaneen (Fig. 1). The site is located in the South African lowveld, in a riverine, subtropical savanna environment situated at 650 m above sea level. The annual rainfall at the closest weather station (Polokwane) is approximately 500 mm, of which 90% falls between October and April. Temperatures vary between a daily mean maximum of 28°C in January to a daily mean minimum of 4°C in July (South African Weather Service). Some frost is experienced during the winter months. The precipitation and temperatures may be slightly higher at the *B. salicina* growth site than in Polokwane, because it is located at a lower altitude than the weather station.

The first tree investigated (M1) grew in alluvial soil, approximately 100 m from the Murle Brooks River, which normally flows all year round, but may dry up during extreme droughts. The river plain is used for commercial fruit plantations, and M1 grew among sparsely planted mango trees, until it fell over during a storm in 1994. The second tree (M2) grew on a hillside approximately 1 km from the Murle Brooks River, close to a smaller, seasonal river. The hillside is not used for any agricultural purposes. The tree was cut down in 1995.

We used one cross section, approximately 10 cm thick, from each tree. The maximum distance from pith to bark was 670 mm for M1 and 475 mm for M2. The visible rings along the radii of both trees were counted and measured under a microscope. The number of rings was also calculated by analysing changes in density throughout the radius; this, however, resulted in a different number of rings compared to the 'visual' ring counting (Table 1). AMS radiocarbon dating of the piths of both trees revealed that the number of rings did not match the age in years, meaning that the visible rings were not produced annually or seasonally. Therefore, instead of using the number of rings as an estimate of age, we used 'wiggle-match dating' (WMD) for age modelling. For this purpose, nine samples each from both M1 and M2 were taken for AMS dating (Table 1). In WMD, the fine fluctuations in the ^{14}C calibration curve are used in order to 'calibrate' a series of close radiocarbon dates.[30] The uncalibrated ^{14}C dates' best fit to the southern hemisphe calibration curve[31] serves as an age model. Post-1950 samples were calibrated from bomb radiocarbon data.[32] The growth pattern of the trees was also taken into account when constructing the age model. The AMS dating was performed at the Ångström Laboratory in Uppsala, Sweden.

For $\delta^{13}C$ analysis, wood was extracted by hand using a corer from the 90 outermost, visible rings in M1 and then every 5 to 10 mm (with a 2-mm and a 5-mm corer, respectively) along a growth radius perpendicular to the growth direction. For very thin rings, drilling was performed over two or more adjacent rings. Samples from M2 were drilled every 5 mm (with a 2-mm corer) from bark to pith, and cellulose was extracted from the raw wood samples. This process involved the removal of oils and resins by extraction in toluene and ethanol. The samples from M1 were processed in a Soxtec HT2 (Perstorp Analytical Tecator) instrument for 8 hours in toluene/ethanol (2:1) solution followed by 8 hours in ethanol only. Samples from M2 were processed in an ASE (accelerated solvent extractor) under high pressure for 2 hours in toluene/ethanol and ethanol, respectively. After drying and placing in plastic tubes, the samples were boiled in water for 5 hours in a water bath. This was followed by oxidation of the lignin constituents in the wood (bleaching), where samples were treated in a water/sodium chlorate/glacial acetic acid solution at 70°C until they turned completely white. After several rinses, the cellulose was oven dried at 50°C and 1.5 mg of each sample was weighed for isotope ratio measurements. The samples were analysed at the Department of Geology and Geochemistry, Stockholm University, using a Finnigan Delta Plus mass spectrometer (equipped with a Carlo Erba NC2500 and conflo interface), with a precision of ±0.2‰.

For the study of density and vessel properties, radial sections were sawn from the discs, parallel to the samples taken for $\delta^{13}C$ analysis. For density measurements, a 2.5-mm-thick strip of the radial section was scanned by a gamma-ray densitometer at continuous steps of 0.5 mm. The same strip was used in the analysis of vessel properties. After saturation in water to soften them, the strips were sectioned into 30-μm-thick transverse slices and mounted in glycerine on glass slides. Vessel properties were recorded continuously every 1 mm along the sections using a fluorescent microscope and a Leica image analysis system. The following parameters were measured: *radial and tangential vessel diameter,* representing the mean averaged radial and tangential diameter of all measured vessels within each sampled area (1 ± 0.9 mm); *vessel percentage,* representing the area occupied by vessels within the measured area; and *vessel frequency,* representing the number of vessels within each measured area. To translate density measurements into ring counts, density changes greater than 0.01 g/cm^3 were defined as ring boundaries. Both density and vessel analysis were performed at the CSIR laboratory in Durban, South Africa.

[c]Synonyms: *Breonadia microcephala, Adina microcephala* var. *galpinii.* Common names: Matumi, Mingerhout, Water Matume, African teak, mohlomê, umHlume. Family: Rubiaceae (Gardenia).

Table 1. Radiocarbon ages and calibrated ages after WMD (wiggle match dating) of wood samples from radii of the two *Breonadia salicina* trees, M1 and M2. Different numbers of rings were included for different ^{14}C samples. The number of tree rings between ^{14}C samples was counted from microscope studies ('visible rings') and from density measurements ('density rings'). 'Missing rings' indicate the difference between the number of years between ^{14}C dates according to WMD, and the number of 'visible rings' between ^{14}C dates. The final calibration dates lie within a 2σ intercept of the calibration curve, except for Ua–20757 in M1 and Ua-22056 in M2, which both lie within the 3σ interval.

M1

^{14}C laboratory number	Location (mm fr. bark)	Rings per date	^{14}C age(yr BP)	^{14}C calibration intercepts, 2σ (yr AD)	Wiggle match date (yr AD)	Years between dates**	'Visible rings' between ^{14}C dates	'Density rings between ^{14}C dates	'Missing rings' between ^{14}C dates
Ua–20758	30	2	148.5 ± 0.5*	1963 1971/72	1963	31	15	15	–16
Ua–20757	100	3	60 ± 35	1824-1826†	1825	138	22	29	–116
Ua–22870	142	1	155 ± 40	1674-1742 1800–1955	1700	125	16	15	–109
Ua–20756	207	4	350 ± 35	1465 1483-1645	1630	70	20	22	–50
Ua-20755	266	2	465 ± 40	1463–1607	1605	25	25	22	0
Ua-20754	328	1	385 ± 35	1457–1636	1585	20	20	30	0
Ua–19434	436	1	365 ± 35	1461–1643	1523	62	62	56	0
Ua–19435	570	1	395 ± 35	1455–1630	1498	34	34	38	0
Ua–20753	670	pith	435 ± 35	1447–1505 1590–1618	1447	42	45	24	3
					Total	**547**	**259**	**251**	**–288**

M2

^{14}C laboratory number	Location (mm fr. bark)	Rings per date	^{14}C age(yr BP)	^{14}C calibration intercepts, 2σ (yr AD)	Wiggle match date (yr AD)	Years between dates**	'Visible rings' between ^{14}C dates	'Density rings' between ^{14}C dates	'Missing rings' between ^{14}C dates
Ua–22053	32	2	156.6 ± 0.7*	1964 1968/69	1968	21	15	10	–11
Ua–22054	82	4	102.4 ± 0.5*	1956/57	1956	16	25	23	12
Ua–22055	112	3	115 ± 35	1700–1726 1808–1955	1895	31	17	14	–44
Ua–21712	127	4	155 ± 35	1675–1740 1800–1955	1840	55	5	7	–50
Ua–22056	157	1	95 ± 30	1715† 1814–1832† 1885–1933†	1715	125	14	13	–111
Ua–22871	191	2	305 ± 40	1507–1587 1619–1667	1640	75	17	19	–58
Ua–22872	222	2	345 ± 40	1484–1648	1565	75	18	13	–57
Ua–21711	332	2	425 ± 40	1448–1510 1551–1559 1579–1622	1470	95	56	51	–39
Ua–20759	475	3 + pith	775 ± 40	1225–1297 1365–1377	1375	95	70	58	–25
					Total	**620**	**237**	**208**	**–383**

*Percent modern carbon (pMC). Calibrated by bomb radiocarbon data.[32]
**According to dates calibrated by wiggle match dating.
†3σ calibration intercept ranges.

Results

Age model for M1

The radius of M1 consisted of 259 visible rings and 251 rings according to density measurements (Table 1). The ring structure close to the pith was distinctive and easily visible to the naked eye, while the structure was vaguer closer to the bark. Nine samples from M1 were AMS dated (Table 1). The chosen age model and concordant growth model are illustrated in Fig. 2. The older, fast-growing (2.5 mm/yr) phase of the tree was dated by placing the radiocarbon dates along the calibration curve at a distance coinciding with the number of visible rings between the dated samples. Hence, for this part of the tree the age model is based on both ring counts and ^{14}C dates. This phase was fixed by the AD 1605 date, which must fit the peak in the radiocarbon calibration curve at this time. At some stage between 1630 and 1700, growth slowed, to reach its minimum (0.3 mm/yr) between 1700 and 1825. It is possible that the tree actually stopped growing for a number of years during this period. After this, the tree grew again, slightly faster, especially during the last 50 years (0.9 mm/yr). During the phases of slow growth, the number of visible rings between the ^{14}C dates does not match the number of years recorded from WMD. A total of 291 rings are missing between 1630 and 1994. For this sequence, we interpolated linearly between the ^{14}C dates to obtain the age model.

Age model for M2

In the second tree, a total of 237 rings were counted from microscope studies and 208 were identified from density changes (Table 1). Nine samples along the radius were AMS dated (Table 1). The growth pattern of M2 is similar to M1's, starting with high growth rates (1.5 mm/yr) during the early stages of the tree's life (Fig. 2). After AD 1565, the growth rate decreased (0.3 mm/yr) and stayed low until the early 1900s, when it increased again with a growth peak during the second half of the century (2.3 mm/yr). The two oldest ^{14}C dates were, as for M1, adjusted to the number of visible rings between the ^{14}C-dated samples. The rings in this section of the tree are very

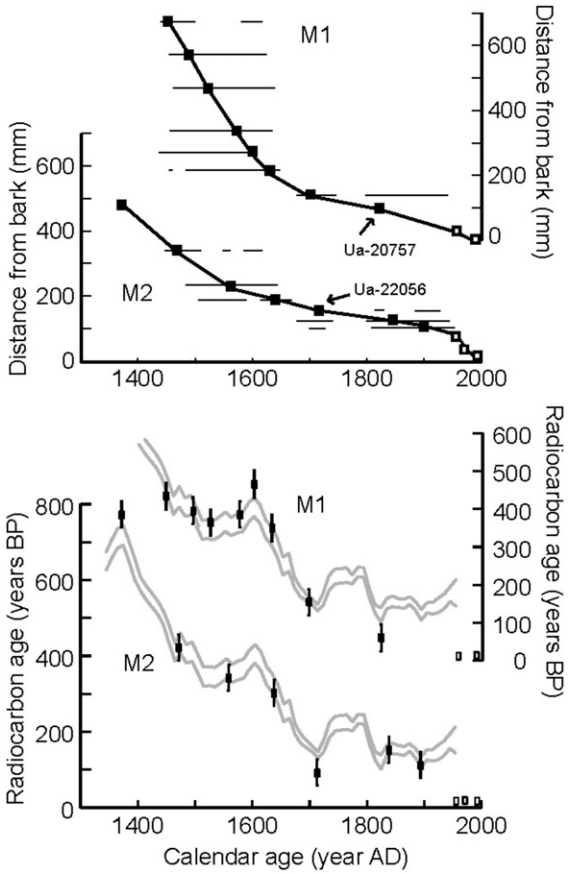

Fig. 2. Growth models (**top**) and ^{14}C wiggle-match dating (**bottom**) for the two *Breonadia salicina* trees, M1 and M2. The growth models show the calibrated dates used in the final age model (■) and their 2σ intercepts (see also Table 1). The oldest date for M2 has an additional intercept outside the presented scale, at AD 1225–1297. Two dates, Ua-20757 in M1 and Ua-22056 in M2, arrowed in the upper graphs, lie within 3σ of the calibration curve, and for these dates the 3σ intercept ranges are also presented (see also Table 1). A radiocarbon calibration curve for the southern hemisphere was used for the wiggle-match dating,[31] here plotted with 2σ. Felling dates (1994 and 1995) as well as the modern ^{14}C samples (post-1955, calibrated by using bomb radiocarbon data,[32] see Table 1) are indicated as unfilled squares (□) in both growth models and wiggle-match dating graphs.

clear and easily identifiable compared to the rings closer to the bark. However, 25 rings are still missing between the two oldest ^{14}C dates. A best fit to the calibration curve and estimates of a plausible growth model served as a basis for the final age model. For the modern date, Ua-22053, which has two intercepts with a 4-year difference, the date corresponding to the smoothest growth curve was chosen. This was also applied to Ua-20758 in M1. A total of 383 rings are missing for the whole sequence, most of them during the 1700s and 1800s, when growth was slowest.

Stable carbon isotopes and wood anatomy

Figure 3 shows the variation in $\delta^{13}C$ values for M1 and M2 and the vessel properties for M2, plotted against the proposed age model. The absolute $\delta^{13}C$ values for M1 varied between –25.1 and –23.3‰, whereas the variation for M2 was greater, ranging between –24.7 and –21.4‰. The mean $\delta^{13}C$ value was –24.1‰ for M1 and –23.1‰ for M2. Because of the continuously more negative $\delta^{13}C$ composition of atmospheric CO_2 since approximately AD 1800, the $\delta^{13}C$ records for both M1 and M2 may be corrected by approximately +1.4‰ since around 1800.[33] For both trees, this correction results in a slightly increasing trend in $\delta^{13}C$ with time throughout the sampled period (grey curves in Fig. 3).

Wood anatomy was successfully analysed throughout the radial section in M2, whereas major parts of the radius of the other tree could not be analysed because of a marked spiral pattern, due to non-vertical growth, of the fibres and vessels. The results from M2 show a clear correlation between the radial vessel diameter and tangential vessel diameter ($r = 0.83$ for M2 and 0.69 for the section of M1 that was successfully analysed). Gillespie *et al.*[26] suggest that the *radial* vessel diameter is a better mirror of rainfall than *tangential* vessel diameter in *B. salicina*. We therefore choose to discuss only the radial diameter in this report. The radial vessel diameter and vessel frequency of M2 are plotted in Fig. 3. Mean radial vessel diameter was 119 μm and mean frequency was 18 vessels per mm^2.

Discussion

The results from both the wiggle-match dating and the pattern of growth structure demonstrate that the experimental trees did not produce visible rings each year since they started growing in the 15th and 14th centuries. During periods of rapid growth, annual rings were formed, whereas a large number of rings are missing in sequences represented by slow growth. It has been shown[13] that subtropical trees can survive episodes of dormancy during times of environmental stress and then start to grow again when conditions are more favourable. Whether the trees in this study experienced significant periods of non-growth or whether they grew continuously, but with such a slow rate of growth that the seasonal rings are too thin for identification, is a question that needs to be investigated further. The present age model is thus more accurate for periods of rapid growth; in other words, for the innermost parts of the trees that were produced when the trees were young, e.g. the period dated to AD 1447–1630 for M1. The age model is less precise during periods of slow growth, found in the parts produced when the trees were older, e.g. the post-1700 period for both M1 and M2.

In general, the $\delta^{13}C$ variations in M1 and M2 show similar trends, although they differ in absolute values (Fig. 3). The differences in absolute values may be a result of micro-environmental or genetic differences between the trees, but they may also indicate that the carbon isotope discrimination in the wood was influenced by the difference in water availability between the two growth sites. M2, which shows larger absolute variations, grew on a hill slope, where soil moisture availability probably varied in accordance with precipitation. M1 grew in a cultivated riparian zone close to a river with an all-year-round water supply. Consequently, the tree was probably not influenced by changes in precipitation amounts to the same extent as M2. Further, M1, which is thought to be the less moisture-stressed tree, shows more-depleted $\delta^{13}C$ values than M2. However, a study of South African pine trees growing at varying distances from a river provides contradictory results; the trees growing close to the river manifest higher $\delta^{13}C$ values than do trees located on hilltops farther away from the river.[16] Thus, more negative $\delta^{13}C$ values, as found for M1 compared to M2, do not necessarily indicate that a tree has been less water stressed. However, all the pine trees in the study by Woodborne[16] responded in a similar way in terms of the relative increase/decrease of $\delta^{13}C$ between years, and these temporal $\delta^{13}C$ variations also corresponded with rainfall.

If the different ranges in absolute $\delta^{13}C$ values between trees are ignored, the temporal changes in carbon isotope composition of the two trees show many similar features (Fig. 3). Both trees display depleted values at around AD 1475, followed by an increase until the mid-1500s. (Note the reversed axis in the $\delta^{13}C$ graph in Fig. 3; depleted $\delta^{13}C$ values are illustrated as peaks, high values as troughs.) Depleted $\delta^{13}C$ values during the 1600s in both

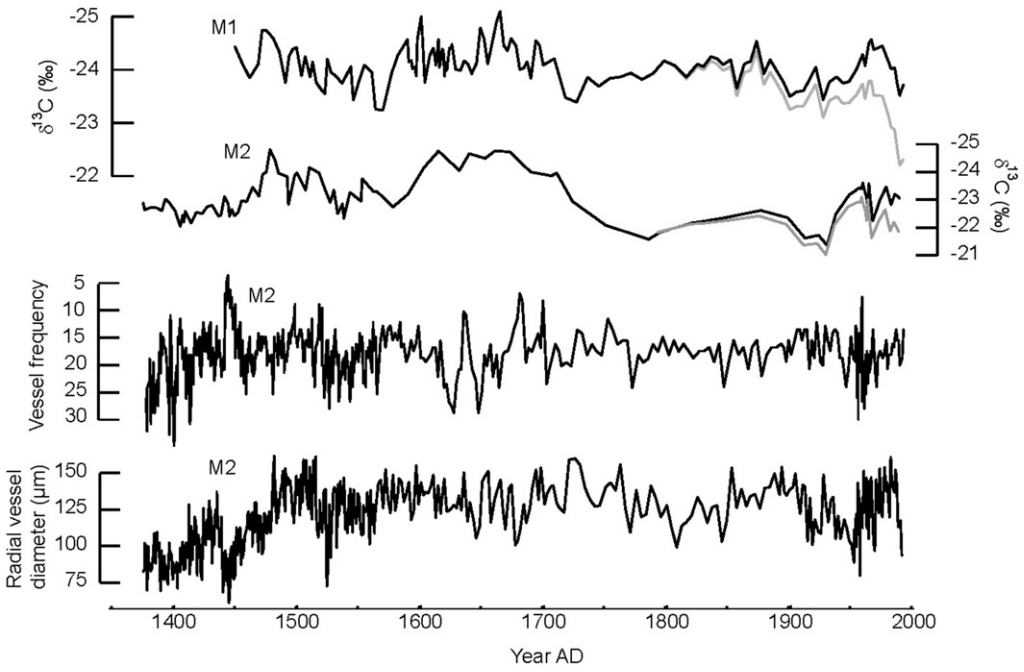

Fig. 3. Variations in carbon isotope composition and vessel properties for *Breonadia salicina*. From top: $\delta^{13}C$ values for M1, $\delta^{13}C$ values for M2, vessel frequency for M2 and radial vessel diameter for M2. All parameters were plotted without filtering. Vessel frequency was measured as the number of vessels per mm^2. Grey curves indicate $\delta^{13}C_{tree}$ corrected for declining $\delta^{13}C_{atm}$ since the 19th century.[33] The low time resolution for *B. salicina* (M2) during the 18th and 19th centuries is due to the slow growth and/or dormancy during this period. Note the reversed *y*-axis in the graphs for $\delta^{13}C$ and vessel frequency.

records are followed by an increase starting at around 1700 and culminating at around 1730 for M1 and at 1790 for M2. During the 1900s, M1 and M2 also show similar trends, with less negative $\delta^{13}C$ values during the first half of the century and during its last decades, while more negative $\delta^{13}C$ values are observed for the mid-1900s for both trees. These correlated trends for both trees suggest that the variations in $\delta^{13}C$ composition in M1 and M2 result from an influence by a common source, although the trees grew at different localities.

Figure 4a shows the $\delta^{13}C$ variations in M1 and M2 during the last century, plotted together with a regional precipitation index and the mean annual rainfall record for Polokwane, stretching back to 1904. The different time-resolutions in the rainfall record and the $\delta^{13}C$ records, together with the limits of the age model during this time sequence, make it difficult to perform an ultimate comparative analysis between parameters on an annual basis. However, some connections between the two parameters can be noted. The $\delta^{13}C$ record covering the last century shows that the highest values (troughs in graph) occur during the early decades, and the most negative $\delta^{13}C$ values occur between 1960 and 1980 in both M1 and M2 (Fig. 4a). According to Polokwane rainfall data, the first half of the 1900s was punctuated by several extreme dry years in the region, especially 1904, 1918 and 1934, while during the second half of the century the rainfall was less variable with a higher annual mean and three extreme wet years in 1955, 1958 and 1964. This supports a weak negative correlation between $\delta^{13}C$ and annual rainfall. Even though a $\delta^{13}C$ series with higher sample resolution would have been preferred, these results suggest a stomatal response to water stress in *B. salicina.* The water stress of the tree is regulated by the soil water availability, which in turn is influenced by rainfall.

In Fig. 4b the vessel properties of both trees during the 1900s are plotted with the rainfall records. The correlation coefficient between vessel frequency (grey curve) and vessel diameter (black curve) is $r = -0.31$ for M1 and -0.27 for M2 during the 1900s. A response in vessel properties due to rainfall is evident at least for M1. High water availability in the soil triggers the trees to optimize the water conductivity in the stem by increasing the size of the vessels and, for safety reasons, decreasing the number of vessels in the wood. The major drought occasions during the first half of the century is reflected in the tree as reduced vessel diameter and higher vessel frequency (Fig. 4b). In M1, the variation in the absolute values of vessel properties were greater during this period than in the latter part of the century, when annual rainfall also was less variable. The two occasions corresponding to increased vessel frequency that is evident during this time were probably the result of the dry years of 1966 and 1982. The vessel properties of the second tree, M2, are more difficult to relate to the precipitation record. The dry spells in 1912, 1918, 1934 and 1945 are relatively well-correlated with changes in vessel properties, but the association appears weaker after 1950, with the exception of the dry year of 1994, which resulted in the vessel diameters of both trees being small.

Local anthropogenic environmental factors such as pesticides, fertilizers and pollution may have contributed to the changes in $\delta^{13}C$ during the last few decades. Increased CO_2, ozone or SO_2 concentrations in the air are known to increase $\delta^{13}C$ in plants,[17,34] as is fertilization.[35] These factors related to anthropogenic activity may have enhanced the rise in $\delta^{13}C$ induced by the dry conditions in the late 1900s. Another possible source of error in the $\delta^{13}C$ record is the 'juvenile effect', that influences the $\delta^{13}C$ composition during the first 50 years of a tree's life.[36] Because of changes in canopy thickness, light exposure, leaf area or tree stand density, for example, the wood produced in a young tree may have a correspondingly reduced $\delta^{13}C$ value.[37] The innermost $\delta^{13}C$ values from the *B. salicina* trees should therefore be interpreted with this in mind.

Given the similar features of both $\delta^{13}C$ series, together with indications of both structural and stomatal response to soil moisture during the last century, we suggest that the $\delta^{13}C$ and anatomy records indicate changes in rainfall. From this hypothesis, the $\delta^{13}C$ record (Fig. 3) indicates that major wet spells occurred in the region around AD 1475, on several occasions between 1600 and 1700, and around 1875. Major droughts

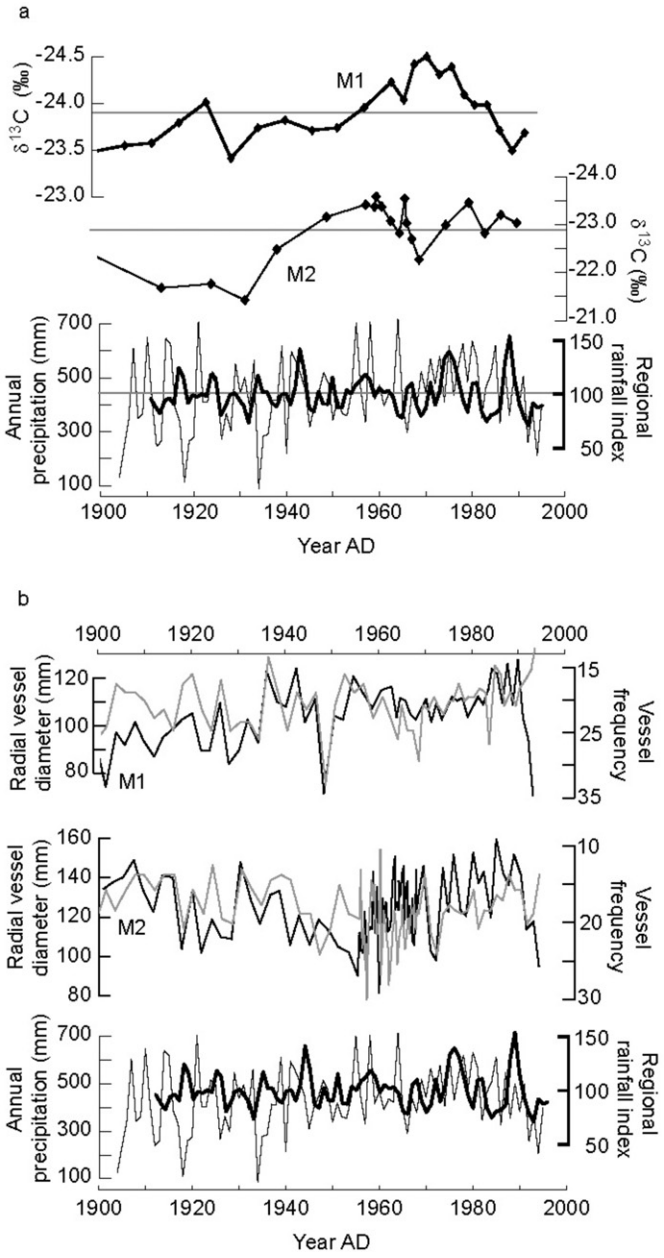

Fig. 4. Properties of M1 and M2 plotted together with rainfall variations at Polokwane weather station and a regional rainfall index (P.D. Tyson, pers. comm.) for the summer rainfall region of South Africa, expressed as a percentage of mean rainfall 1960–90. Horizontal lines represent the mean $\delta^{13}C$ composition and mean annual rainfall, respectively. **a**, Upper two graphs: $\delta^{13}C$ composition (raw values) for *Breonadia salicina*. Lower graph: Annual mean precipitation (thin line) and 2-year running mean of the regional rainfall index (bold). **b**, Upper two graphs: vessel properties of *B. salicina*. Vessel frequency plotted in grey (with reversed axis) and radial vessel diameter plotted in black. The vessel frequency is expressed as the number of vessels per mm^2. Lower graph: annual mean precipitation (thin line) and 2-year running mean of the regional rainfall index (bold).

occurred during years prior to 1475, and around 1540, 1575, 1720 and 1780. Unfortunately, we do not have a complete record of wood anatomy for M1 — the tree that best correlated vessel data with rainfall in the 1900s. The vessel diameter and frequency data from M2 indicate that dry periods occurred at around AD 1400, 1450, 1530, 1650, 1775 and 1850.

The *B. salicina* record shows similarities with other palaeoclimatic records for South Africa. In mid-1400, when the *B. salicina* record indicates small vessel diameter and enriched $\delta^{13}C$ values, followed by increasing vessel diameter and depleted isotope values at around 1500, speleothem isotope records from the Makapansgat Valley (about 100 km southwest of the M1 site) show a change from cold, dry conditions to warmer, wetter ones.[6] The trend towards a slow growth rate, smaller vessels and enriched $\delta^{13}C$ values starting at around 1700 in *B. salicina* is contemporary with changes in regional climate observed in several studies from Africa.[5–8,15,38] Makapansgat speleothems indicate certain dry and cold conditions during the 1700s and a tree-ring record from the Karkloof forest in KwaZulu-Natal suggest lower rainfall levels in the region from early 1700 until about 1800.[38] During the 1800s, the $\delta^{13}C$ values in *B. salicina* decreased again, followed by a rise in early 1900. Both the Karkloof tree record and the Makapansgat speleothem record indicate wet conditions in the 1800s. This close similarity with other palaeoclimatic records from the region is an additional indication that $\delta^{13}C$ composition is dominated by a stomatal response to moisture stress, and that depleted $\delta^{13}C$ values, large vessel diameter and high growth rate indicate regionally wetter conditions, whereas enriched $\delta^{13}C$ values, small vessel diameter and slow growth signify regionally drier conditions.

Conclusions

By studying the subtropical tree *Breonadia salicina,* we retrieved a greater than 600-year record of changes in moisture-sensitive parameters, even though this tree does not reveal continuously visible annual rings. Through closely spaced ^{14}C dating and wiggle-matching, a fairly good age model was obtained. The two trees analysed span the period AD 1375–1995 and show variations in $\delta^{13}C$ values, vessel diameter, vessel density and growth rate. The similarities between previous palaeoclimate records, the instrumental rainfall record and our data support the hypothesis that the changes in the *B. salicina* record regarding $\delta^{13}C$ composition, vessel diameter and growth rate are governed by changes in the trees' access to water because of variations in regional rainfall. We therefore interpret depleted $\delta^{13}C$ values, large vessel diameter and fast tree growth as indicating regionally wetter conditions; enriched $\delta^{13}C$ values, small vessel diameter and slow growth correspond to regionally drier conditions. Important features of the *B. salicina* record are the occurrence of a drier than average phase during the mid-1500s, followed by wetter conditions during the 1600s. A dry period in the 1700s was followed in the 1800s by slightly wetter conditions.

A future study would benefit from the use of several *B. salicina* trees as well as by closer sampling for both AMS dates and $\delta^{13}C$ analysis. Such a study has the potential to produce an even more detailed analysis, with a time resolution of up to a decade, of past regional climate in northern South Africa, a region where long, continuous and high-resolution climate records are rare.

We thank Peter Tyson (University of the Witwatersrand, Johannesburg) for initiating this project and for supplying us with the Matumi wood sections. We also thank Ed February (University of Cape Town) for advice regarding the laboratory process, and Stephan Woodborne (CSIR, Pretoria) for organizing the vessel and density analysis, and for general discussions. Hans Linderholm, Stephan Woodborne, Ann-Marie Robertsson and an anonymous referee all helped to improve the manuscript. The AMS dates were analysed by Göran Possnert at the Ångström Laboratory, Uppsala. The project is financed by the Swedish International Development Cooperation Agency (SIDA), with additional support from the Swedish Association for Anthropology and Geography (SSAG), the Carl Mannerfelt's Fund, the Axel Lagrelius' Fund for Geographic Research and the Ahlmann Fund.

Received 3 January. Accepted 20 April 2005.

1. IPCC (2001). *Climate Change 2001: The Scientific Basis.* Contribution of Working Group I to the Third Assessment Report of the Intergovernmental Panel on Climate Change (IPCC), Technical Summary. Geneva.
2. Stott L., Poulsen C., Lund S. and Thunell R. (2002). Super ENSO and global climate oscillations at millennial time scales. *Science* **297**, 222–226.

3. Schmidt M.W., Spero H.J. and Lea D.W (2004). Links between salinity variation in the Carribean and North Atlantic thermohaline circulation. *Nature* **428**, 160–163.
4. Turney C.S.M, Kershaw A.P., Clemens S.C., Branch N., Moss P.T. and Fifield L.K. (2004). Millennial and orbital variations of El Niño/Southern Oscillation and high-latitude climate in the last glacial period. *Nature* **428**, 306–310.
5. Talma A.S. and Vogel J.C. (1992). Late Quaternary paleotemperatures derived from a speleothem from Cango Caves, Cape Province, South Africa. *Quat. Res.* **37**, 203–213.
6. Holmgren K., Lee-Thorp J.A., Cooper G., Lundblad K., Partridge T.C., Scott L., Sithaldeen R., Talma A.S. and Tyson P.D. (2003). Persistent millennial-scale climatic variability over the past 25 000 years in southern Africa. *Quat. Sci. Rev.* **22**, 2311–2326.
7. Scott L. (1996). Palynology of hyrax middens: 2000 years of palaeo-environmental history in Namibia. *Quat. Int.* **33**, 73–79.
8. Johnson T., Barry S., Chan Y. and Wilkinson P. (2001). Decadal record of climate variability spanning the past 700 yr in southern tropics of East Africa. *Geology* **29**, 83–86.
9. Stahle D.W., Mushove P.T., Cleaveland M.K., Roig F. and Haynes G.A. (1999). Management implications of annual growth rings in *Pteocarpus angolensis* from Zimbabwe. *Forest Ecol. Mngmt* **124**, 217–229.
10. Andronova N.G., Schlesinger M.E. and Mann M.E. (2004). Are reconstructed pre-instrumental hemispheric temperatures consistent with instrumental hemispheric temperatures? *Geophys. Res. Lett.* **31**, art. no. L12202.
11. Fritts H.C. (1976). *Tree Rings and Climate.* Academic Press, London.
12. Lilly M.A. (1977). *Environmental studies: An assessment of the dendrochronological potential of indigenous tree species in South Africa.* Occasional paper no. 18, Department of Geography and Environmental Studies, University of the Witwatersrand, Johannesburg.
13. Détienne P. (1989). Appearance and periodicity of growth rings in some tropical woods. *IAWA Bull.* **10**, 123–132.
14. Jacoby G. (1989). Overview of tree-ring analysis in tropical regions. *IAWA Bull.* **10**, 99–108.
15. Dunwiddie P.W. and LaMarche V.C. Jr. (1980). A climatically responsive tree-ring record from *Widdringtonia cedarbergensis,* Cape Province, South Africa. *Nature* **286**, 796–797.
16. Woodborne S., Robertson I. and February E. (2003). *The use of isotope* ($\delta^{13}C$) techniques to define the riparian zone in commercially afforested catchments. Report to the Water Research Commission, Project K5/1218/0/1, Pretoria.
17. Farquhar G.D., O'Leary M.H and Berry J.H. (1982). On the relationship between carbon isotope discrimination and the intercellular carbon dioxide concentration in leaves. *Aust. J. Plant Phys.* **9**, 121–137.
18. McCarroll D. and Loader N.J. (2004). Stable isotopes in tree rings. *Quat. Sci. Rev.* **23**, 771–801.
19. Lipp J., Trimborn P., Fritz P., Moser H., Becker B. and Frenzel B. (1991). Stable isotopes in tree ring cellulose and climatic change. *Tellus* **43B**, 322–330.
20. McCarroll D. and Pawellek F. (2001). Stable carbon isotope ratios of *Pinus sylvestris* from northern Finland and the potential for extracting a climate signal from long Fennoscandian chronologies. *Holocene* **11**, 517–526.
21. Hemming D.L., Switsur V.R., Waterhouse J.S., Heaton T.H.E. and Carter A.H.C. (1998). Climate variation and the stable carbon isotope composition of tree ring cellulose: an intercomparison of *Quercus robur, Fagus sylvatica* and *Pinus silvestris. Tellus* **50B**, 25–33.
22. Sonninen E. and Jungner H. (1995). Stable carbon isotopes in tree-rings of a Scots pine (*Pinus silvestris* L.) from northern Finland. In *Problems of Stable Isotopes in Tree-rings, Lake Sediments and Peat-bogs as Climatic Evidence for the Holocene.* Palaeoclimate Research 15. European Palaeoclimate and Man 10, ed. B. Frenzel, pp.121–128. Gustav Fischer Verlag, Mainz.
23. Loader N.J. and Switsur V.R. (1996). Reconstructing past environmental change using stable isotopes in tree-rings. *Bot. J. Scot.* **48**, 65–78.
24. Saß U. and Eckstein D. (1992). The annual vessel area of beech as an ecological indicator. In *International Dendrochronological Symposium on Tree Rings and Environment, Lundqua Report 34,* ed. O. Eggertsson, pp. 281–285. Lund, Sweden.
25. February E.C. (1993). Sensitivity of xylem vessel size and frequency to rainfall and temperature: implications for paleontology. *Paleont. afr.* **30**, 91–95.
26. Gillespie R.D., Sym S.D. and Rogers K.H. (1998). A preliminary investigation of the potential to determine the age of individual trees of *Breonadia salicina* (Rubiaceae) by relating xylem vessel diameter and area to rainfall and temperature data. *S. Afr. J. Bot.* **64**, 316–321.
27. Tyree M.T. and Zimmermann M.H. (2002). *Xylem Structure and the Ascent of Sap.* Springer-Verlag, Berlin.
28. Coates Palgrave K. (1983). *Trees of Southern Africa.* Struik, Cape Town.
29. van Wyk B., van Wyk P. and van Wyk B-E. (2000). *Photographic Guide to Trees of Southern Africa.* Struik, Cape Town.
30. Blaauw M. (2003). *An investigation of Holocene sun-climate relationships using numerical C-14 wiggle match dating of peat deposits.* Ph.D. thesis, University of Amsterdam, Holland.
31. McCormac F.G., Reimer P.J., Hogg A.G., Higham T.F.G., Baille M.G.L., Palmer J. and Stuvier M. (2002). Calibration of the radiocarbon time scale for the southern hemisphere: AD 1850–950. *Radiocarbon* **44**, 641–651.
32. Vogel J.C., Fuls A. and Visser E. (2002). Accurate dating with radiocarbon from the atom bomb tests. *S. Afr. J. Sci.* **98**, 437–438.
33. Francey R.J., Allison C.E., Etheridge D.M., Trudinger C.M., Enting I.G., Leuenberger M., Langenfelds R.L., Michel E. and Steele L.P. (1999). A 1000-year high precision record of $\delta^{13}C$ in atmospheric CO_2. *Tellus* **51B**, 170–193.
34. Martin B. and Southerland E.K. (1990). Air pollution in the past recorded in width and stable carbon isotope composition of annual growth rings of Douglas-fir. *Plant, Cell Environ.* **13**, 839–844.
35. Livingston N.J., Guy R.D., Sun Z.J. and Ethier G.J. (1999). The effect of nitrogen stress on the stable carbon isotope composition, productivity and water use efficiency of white spruce (*Picea glauca* (Moench) Voss) seedlings. *Plant, Cell Environ.* **22**, 281–289.
36. Freyer H.D. and Belacy N. (1983). $^{12}C/^{13}C$ records in northern hemispheric trees during the past 500 years: anthropogenic impact and climatic superpositions. *J. Geophys. Res.* **88**, 6844–6852.
37. Francey R.J. (1986). Carbon isotope measurements in baseline air, forest canopy air and plants. In *The Changing Carbon Cycle — A global analysis,* eds J.R. Trabalka and D.E. Reichle, pp. 160–174. Springer Verlag, New York.
38. Hall M. (1976). Dendroclimatology, Rainfall and human adaption in the later Iron Age of Natal and Zululand. *Ann. Natal Mus.* **22**, 693–703.